Vol 15 No 11, November 2006
1009-1963/2006/15(11)/2688-09
Chinese Physics
© 2006 Chin. Phys. Soc.
and IOP Publishing Ltd

Study on the mixing of fluid in curved microchannels with heterogeneous surface potentials*

Lin Jian-Zhong(林建忠)[a)b)†], Zhang Kai(张 凯)[a)], and Li Hui-Jun (李惠君)[a)]

[a)] *Department of Mechanics, State Key Laboratory of Fluid Power Transmission and Control, Zhejiang University, Hangzhou* 310027, *China*

[b)] *China Jiliang University, Hangzhou* 310018, *China*

(Received 26 March 2006; revised manuscript received 12 May 2006)

In this paper the mixing of a sample in the curved microchannel with heterogeneous surface potentials is analysed numerically by using the control-volume-based finite difference method. The rigorous models for describing the wall potential and external potential are solved to get the distribution of wall potential and external potential, then momentum equation is solved to get the fully developed flow field. Finally the mass transport equation is solved to get the concentration field. The results show that the curved microchannel has an optimized capability of sample mixing and transport when the heterogeneous surface is located at the left conjunction between the curved part and straight part. The variation of heterogeneous surface potential $\psi_{\rm n}$ has more influence on the capability of sample mixing than on that of sample transport. The ratio of the curved microchannel's radius to width has a comparable effect on the capability of sample mixing and transport. The conclusions above are helpful to the optimization of the design of microfluidic devices for the improvement of the efficiency of sample mixing.

Keywords: microchannel, mixing efficiency, electroosmosis, numerical simulation
PACC: 6740H, 8265F, 4760

1. Introduction

With the development of micro-system technology, it is common that the electro-osmosis is utilized as one of the driving forces for fluid transport and mixing simultaneously in microchannels, and more attentions have been paid to the relation between the characteristics of microchannel and the efficiency of sample mixing. In general, the Reynolds number of electro-osmotic flow in microfluidic devices is usually very small, and the achievement of sufficient mixing in electro-osmotic microchannel flow is usually very difficult. Though a longer mixing length does not mean a sufficient mixing,[1] it is still usually used as a method for adding to sample mixing, and curved part is often introduced into a narrow microchannel. Then, it is very important to have a study on sample mixing in curved microchannel. In fact, a lot of work has already been done on the mixing in pressure-driven microchannel,[2−6] and it was found that higher Re number means more sufficient sample mixing.

In general, the manners of sample mixing in microchannels are classified into two categories: diffusion and convection. For a sample with constant molecular diffusion coefficient, lowering its velocity may have more sufficient sample mixing, which is adapted to the sample mixing in straight or curved microchannel. However, in some conditions, both rapid transport and mixing of sample are required. As a result, it should be thought much of the positive influence of convection on sample mixing.

In recent years, Ajdari[7,8] investigated electroosmosis with nonuniform surface potential and found circulation regions generated by application of oppositely charged surface heterogeneities to the microchannel wall. Fu *et al*[9] found that a step change in zeta potential caused a significant variation in the velocity profile and in the pressure distribution. The phenomena were also observed experimentally by Stroock *et al*[10] and Erickson and Li,[11] and they studied these circulation regions and exploited them as a method for the enhancement of mixing in T-shaped microfluidic device. Oddy *at al*[12] used a sinusoidally alternating electric field to stir the flow stream, and Hao *et al*[13] exploited the instability of electrokinetic microchannel flows with conductivity gradients to enhance sample mixing. From the afore-

*Project supported by the National Natural Science Foundation (Grant No 10372090) and the Doctoral Program of Higher Education of China (Grant No 20030335001).
†Corresponding author. E-mail: jzlin@sfp.zju.edu.cn

mentioned works of some researchers, it can be seen that the instability of flow field and circulation regions can be utilized to add sample mixing in some degree, but for a microchannel, there is a tradeoff between the capability of sample mixing and transport.[14]

The integral capability of sample mixing and transport for a microchannel is called its efficiency of sample mixing. Unfortunately, this efficiency of sample mixing for a microchannel has not been well understood. Therefore, numerical simulation will be used to understand the relation between the efficiency of sample mixing and the distribution of heterogeneous wall, wall potential, and the shape of microchannel.

2. Mathematical model and boundary conditions

2.1. Mathematical model

The curved microchannel with width W, radius r and a straight length l is shown in Fig.1. Assuming that the flow is incompressible and steady, we can obtain the momentum equation of flow as:

$$\rho(\boldsymbol{V}\cdot\nabla)\boldsymbol{V} = -\nabla p + \mu\nabla^2\boldsymbol{V} + \boldsymbol{F}\,, \tag{1}$$

where $\boldsymbol{V}$ is velocity vector, p is pressure, ρ and μ denote the density and the viscosity of the solution respectively.

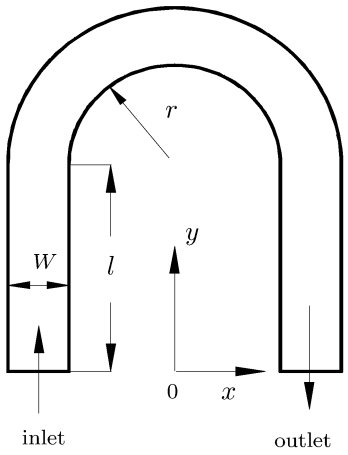


Fig.1. The sketch of computational region.

Based on the property of flow field, two velocity components are described by: $u = u(x, y)$, $v = v(x, y)$. In addition, the flow is driven by electroosmosis, then Eq.(1) can be expressed below:

$$\rho(\boldsymbol{V}\cdot\nabla)\boldsymbol{V} = -\nabla p + \mu\nabla^2\boldsymbol{V} + \rho_{\mathrm{e}}\boldsymbol{E}\,, \tag{2}$$

where $\boldsymbol{E}$ is the electric field, which is given by $\boldsymbol{E} = \nabla\Psi$, and Ψ is the electric potential, ρ_{e} is the charge density. The relation between the net charge density ρ_e and the electrical potential Ψ is shown below:

$$\frac{\partial^2\Psi}{\partial x^2} + \frac{\partial^2\Psi}{\partial y^2} = -\frac{\rho_{\mathrm{e}}}{\varepsilon\varepsilon_0}\,, \tag{3}$$

where ε is the dielectric constant of the electrolyte solution and ε_0 is the permittivity of vacuum.

In general, ion concentration is affected by both the distribution of the externally applied potential, ϕ, and the distribution of the potential, ψ, associated with the electrical double layer (with surface potential, ζ). The overall electric potential, Ψ, is composed of both ϕ and ψ. However, in general, the electrical double layer potential distribution ψ is only a small fraction of Ψ. Since the Debye length (λ_d) is typically very small in comparison with the microchannel height, the ion distribution is influenced primarily by the ζ potential. It is reasonable to assume that the electric potential Ψ is given by the linear superposition of the electrical double layer potential and the externally applied potential, i.e. $\Psi = \psi + \phi$. Therefore, Eq.(3) can be represented as:

$$\frac{\partial^2\psi}{\partial x^2} + \frac{\partial^2\psi}{\partial y^2} = -\frac{\rho_{\mathrm{e}}}{\varepsilon\varepsilon_0}\,, \tag{4}$$

$$\nabla^2\phi = 0\,, \tag{5}$$

where

$$\rho_{\mathrm{e}} = -2n_\infty ze\sinh\Big(\frac{ze\psi}{k_{\mathrm{B}}T}\Big)\,, \tag{6}$$

where z is the valence of ions, e is the fundamental electric charge, n_∞ is the ionic number concentration in the bulk solution, T is the absolute temperature of the solution and k_{B} is Boltzmann's constant. Substituting Eq.(6) into Eq.(2) we get

$$\rho(\boldsymbol{V}\cdot\nabla)\boldsymbol{V} = -\nabla p + \mu\nabla^2\boldsymbol{V} + 2n_\infty ze\sinh\Big(\frac{ze\psi}{k_{\mathrm{B}}T}\Big)\nabla(\psi+\phi)\,. \tag{7}$$

Sample transport in electro-osmotic flows is a result of two primary mechanisms: convection and diffusion. Since steady state is assumed here, the general equation of sample mixing can be written as:

$$(\boldsymbol{V}\cdot\nabla)C = D(\nabla^2 C), \tag{8}$$

where C and D is the sample concentration and diffusivity respectively.

Define $d_{\mathrm{h}} = H$ as the characteristic length, the concentration of sample C_{m} at inlet as the characteristic concentration, an arbitrary velocity U as the

characteristic velocity, and $1/k$ as the characteristic thickness of electrical double layer. Reynolds number $\mathrm{Re} = Ud_\mathrm{h}\rho/\mu$, Schmidt number $\mathrm{Sc} = \mu/D\rho$. The following dimensionless parameters are introduced:

$$u^* = \frac{u}{U}, \qquad C^* = \frac{C}{C_\mathrm{m}},$$
$$\psi^* = \frac{ze\psi}{k_\mathrm{B}T}, \qquad E_x^* = \frac{E_x L}{\zeta},$$
$$x^* = \frac{x}{d_\mathrm{h}}, \qquad y^* = \frac{y}{d_\mathrm{h}},$$
$$\phi^* = \frac{ze\phi}{k_\mathrm{B}T}, \qquad p^* = \frac{(p - p_\mathrm{atm})}{\rho U^2},$$

where ζ is the surface potential on the wall, and p_atm is the atmospheric pressure.

Equations (4), (5), (7) and (8) are non-dimensionalized by above dimensionless variables, the corresponding dimensionless equations can be obtained (with "*" omitted):

$$\nabla^2\psi = (kd_\mathrm{h}^2)\sinh(\psi), \tag{9}$$
$$\nabla^2\phi = 0, \tag{10}$$
$$(\boldsymbol{V}\cdot\nabla)\boldsymbol{V} = -\nabla p + \frac{1}{\mathrm{Re}}\nabla^2\boldsymbol{V} + G_x\sinh(\psi)\nabla(\psi+\phi), \tag{11}$$
$$(\boldsymbol{V}\cdot\nabla)C = \frac{\nabla^2 C}{\mathrm{Sc}\cdot\mathrm{Re}}, \tag{12}$$

where

$$k = \Big(\frac{2n_\infty z^2 e^2}{\varepsilon\varepsilon_0 k_\mathrm{B}T}\Big)^{1/2},$$

and k^{-1} is defined as the Debye length (λ_d), and $G_x = 2n_\infty k_\mathrm{B}T/\rho U^2$.

2.2. Boundary conditions

The present simulation applies the following boundary conditions:
inlet:

$$\frac{\partial\psi}{\partial y} = 0, \quad \phi = \phi_\mathrm{in},$$
$$\frac{\partial u}{\partial y} = 0, \quad \frac{\partial v}{\partial y} = 0,$$
$$C = 0 \quad \text{for} \quad x \le -\frac{r+W}{2W};$$
$$C = 1 \quad \text{for} \quad x > -\frac{r+W}{2W}.$$

outlet:

$$\frac{\partial\psi}{\partial y} = 0, \qquad \phi = \phi_\mathrm{out}, \quad \frac{\partial u}{\partial y} = 0,$$
$$\frac{\partial v}{\partial y} = 0, \qquad \frac{\partial C}{\partial y} = 0$$

on the walls:

$\psi = \psi_\mathrm{n}$ at the wall in one patterned zone;

$\psi = \psi_\mathrm{p}$ at the rest wall of the curved microchannel;

$$\frac{\partial\phi}{\partial\boldsymbol{n}} = 0, \quad u = 0, \quad v = 0, \quad \frac{\partial C}{\partial n} = 0,$$

where $\boldsymbol{n}$ means the local normal of the wall of curved microchannel.

The control-volume-based finite difference method was used to solve the equations above. Equations (9) and (10) were solved first to get the distribution of surface potential and externally applied potential in the microchannel, then Eq.(11) was solved to get a fully developed flow field, Eq.(12) was finally solved by using implicit method to study the sample mixing. The method and code used in present simulation has already been validated.[15,16]

3. Results and discussions

Numerical simulation of the mixing of some type of sample in the curved microchannel was carried out. The present simulation assumes the curved microchannel to be made of silica glass, to have a width of $W = 100$ μm, a straight length of $l = 1$ mm, and its radius changes with r:W. Furthermore, it is assumed that water-liquid is used as the working fluid and its physical properties are given by $\varepsilon = 80$, $\varepsilon_0 = 8.85\times10^{-12}$ C/V$\cdot$ m, $\mu = 1.003\times10^{-3}$ kg/ms, $\rho = 998.2$ kg/m^3. Finally, the diffusion coefficient for sample mixing is $D = 1.0\times10^{-10}$ m^2/s. The characteristic velocity is assumed to be $U = 1$ mm/s. All the numerical solutions presented in the following have been carefully studied so that the grid-independent solutions are obtained.

Referring to Fig.2, we know that each patterned zone is the interaction between the whole curved microchannel and its corresponding dashed rectangular zone respectively. In addition, each patterned zone means a possible region where the wall of the curved microchannel can be modified with heterogeneous surface potential ψ_n, while the rest walls of the curved microchannel have a surface potential ψ_p.

The microchannel has an external electric potential of $\phi_\mathrm{in} = 0$ V and $\phi_\mathrm{out} = 1000$ V, and joule

heating effect can be ignored here. In present study, $\psi_{\rm p} = 0.05$ V, but $\psi_{\rm n}$ is changeable.

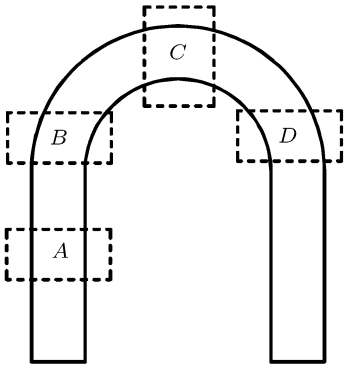


Fig.2. Schematic diagram of the patterned surfaces with heterogeneous surface potential.

In order to make description convenient, some dimensionless parameters are defined as follows:

a) dimensionless theoretical concentration $C_{\rm ideal} = 1.0H_1V_{\rm avg1}/(H_1V_{\rm avg1} + H_0V_{\rm avg0})$, this parameter describes the dimensionless value of concentration at the outlet of the microchannel when complete mixing is achieved without loss, where "1.0" means the stream of sample at the inlet, H_1 and $V_{\rm avg1}$ are sample's corresponding dimensionless length and dimensionless velocity at inlet, other parameters in the above expression above are about working fluid, and they are defined in the same way;

b) dimensionless flux $Q = u(y) \times 1.0$, it is defined to describe sample transport, where "1.0" denotes the dimensionless value of the height of microchannel;

c) mixing parameter

$$\mathrm{Mix}_{\rm eff} = \left(\int_H |C - C_{\rm ideal}|\mathrm{d}H\right) \Big/ (H)\,,$$

this parameter is defined to describe the degree of sample mixing at the outlet of the microchannel, the smaller $\mathrm{Mix}_{\rm eff}$ means the more sufficient sample mixing at the outlet in the curved microchannel and it has been figured out that $C_{\rm ideal}$ is about 0.5 in this simulation.

The present simulation is carried out for the following three cases:

a) the relation between the pattern of the heterogeneous surface and $\mathrm{Mix}_{\rm eff}$, $C_{\rm ideal}$ and Q was investigated when $r{:}\,W = 5 : 1$ and $\psi_{\rm n} = -0.25$ V, the patterned zones of A, B, C and D are defined below:

$$\begin{aligned}
A:&\quad x<0,\quad \frac{l}{2W}<y<\frac{l}{2W}+\frac{r+W}{5W},\\
B:&\quad x<-\frac{4(r+W)}{5W},\quad y>\frac{l}{W},\\
C:&\quad -\frac{(r+W)}{10W}<x<\frac{(r+W)}{10W},\quad y>\frac{l}{W},\\
D:&\quad x>\frac{4(r+W)}{5W},\quad y>\frac{l}{W};
\end{aligned}$$

b) the relation between the heterogeneous surface potential $\psi_{\rm n}$ and $\mathrm{Mix}_{\rm eff}$, $C_{\rm ideal}$ and Q was investigated in the microchannel with the pattern of B and $r{:}W = 5 : 1$;

c) When $\psi_{\rm n} = -0.25$ V, the relation between $r{:}W$ and $\mathrm{Mix}_{\rm eff}$, $C_{\rm ideal}$ and Q was investigated in the microchannel with the pattern of B.

Referring to Figs.3(a)–3(g), we see that there exists circulation region adjacent to heterogeneous surface, in fact, the circulation region is generated by the application of oppositely charged surface heterogeneities to the microchannel wall and its shape can change with the variation of the pattern of heterogeneous surface. In addition, it can also be noted that the circulation region shown in Figs.3(a) and 3(e) is symmetric, but the circulation regions shown in Figs.3(c) and 3(g) are asymmetric, and there is an obvious difference of size between the two adjacent circulation regions.

Referring to Figs.4(a)–4(d), we see that the sample in the curved microchannel with the pattern of B or D can achieve sufficient mixing much easier than that with the pattern of A, and there is almost no mixing in the microchannel with pattern of C. According to Figs.3(b) and 3(f), we can note that the two adjacent circulation regions are confined to half of the width of the microchannel respectively, which means that there is no convection between sample and working fluid. As a result, sample mixing in this kind of curved microchannel can only rely on diffusion, and the terrible sample mixing can be seen in Figs.4(a) and 4(c). Turn to Figs.3(d) and 3(h), it can be found that the outer circulation region has much larger size than the inner circulation region, but the same intensity, which means that the outer circulation will compress one fluid to its adjacent laminar fluid and add to their mutual mixing through convection. As a result, it can be seen in Figs.4(b) and 4(d), that there exists a compression region, before which there is no obvious sample mixing.

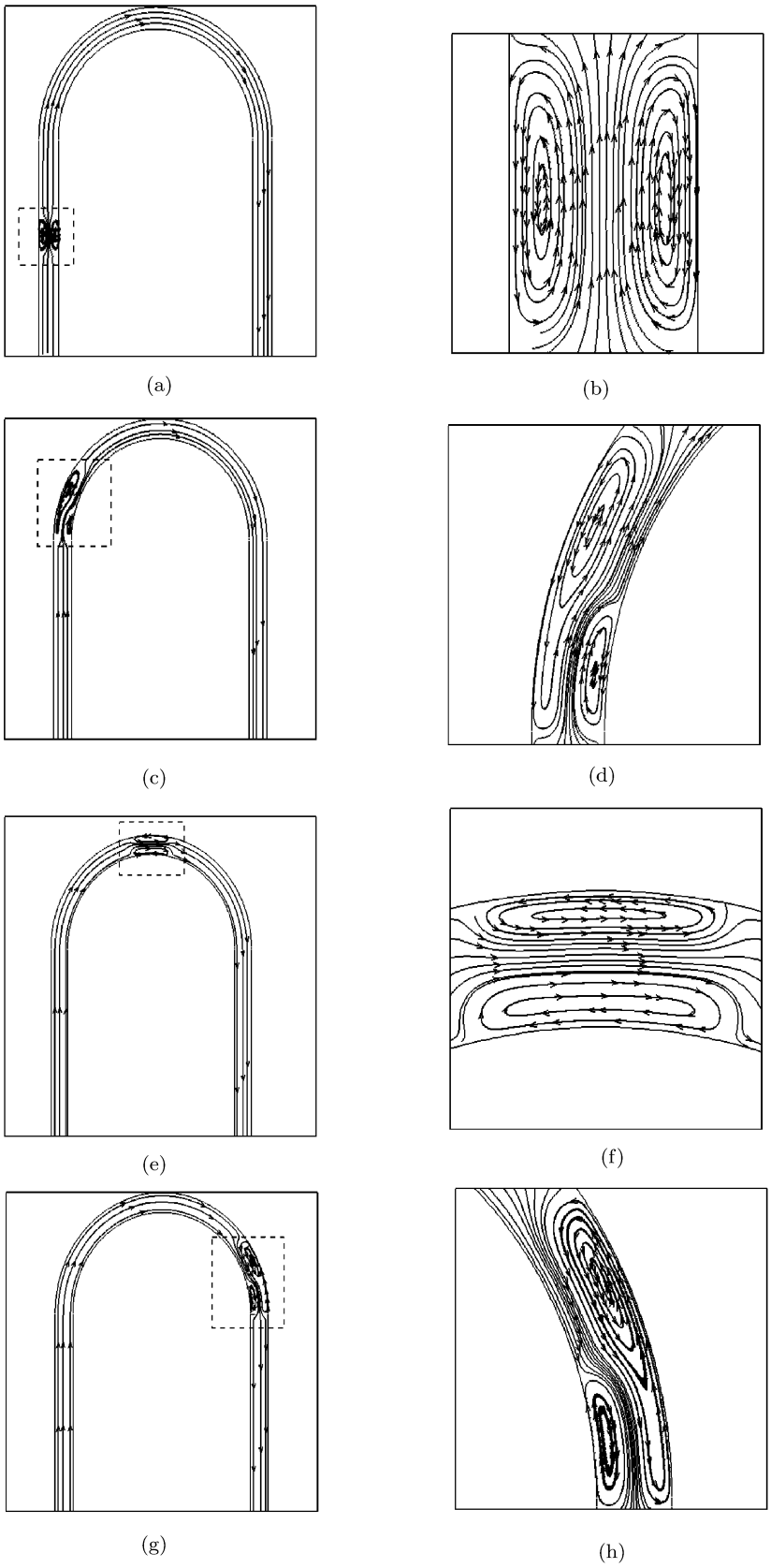


Fig.3. The flow field in the curved microchannel for various pattern of heterogeneous surface potential (a) A, (c) B, (e) C and (g) D when r: $W = 5 : 1$ and $\psi_{\rm n} = -0.25$ V. The flow field shown in Figs.3(b), 3(d), 3(f) and 3(h) is the magnified result of the flow field in the dashed rectangular zone in Figs.3(a), 3(c), 3(e), 3(g) respectively.

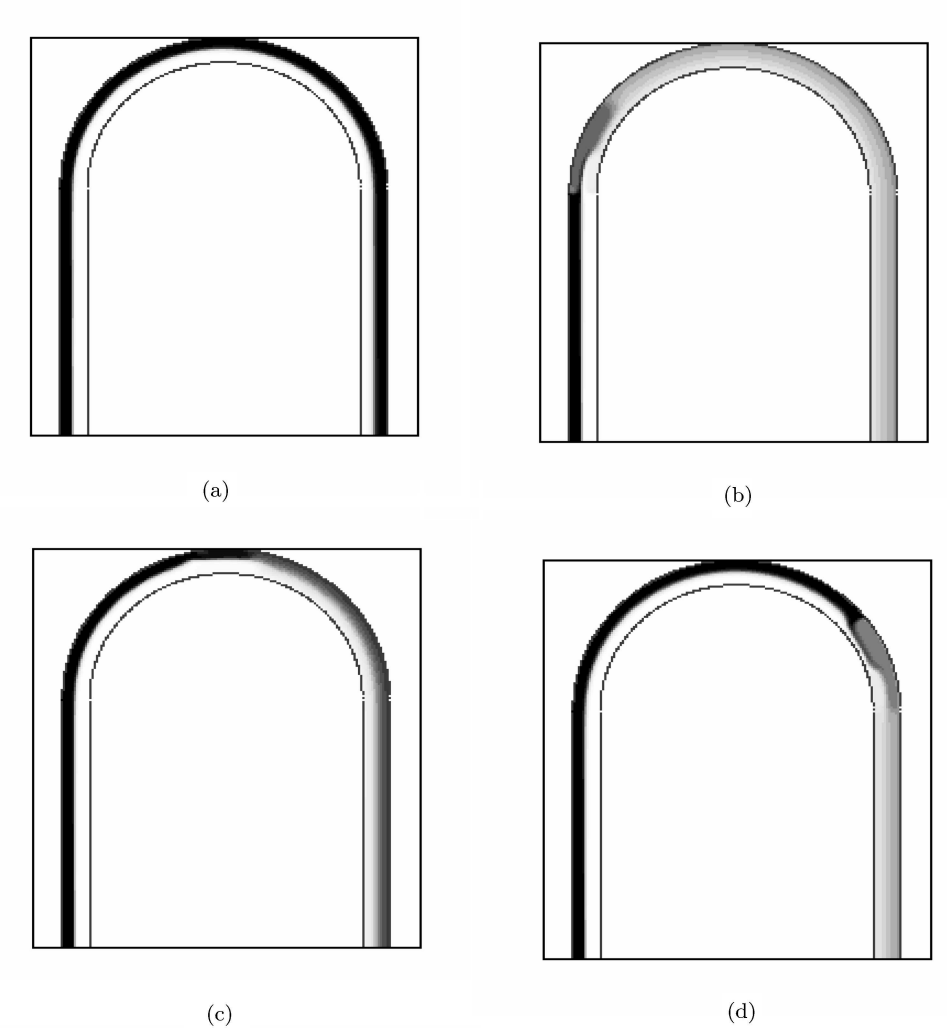


Fig.4. The concentration field in the curved microchannel for various pattern of heterogeneous surface potential (a) A, (c) B, (e) C and (g) D when $r{:}W = 5:1$ and $\psi_{\rm n} = -0.25$ V, where the value of the concentration in the black zone is lower than that in the white zone, and the maximum and minimum value of concentration is 1 and 0, respectively.

As shown in Fig.5(a), it can be seen that the concentration of sample at the outlet of microchannel corresponding to pattern A or C is more uniform than that corresponding to pattern B and D. Referring to Fig.5(b), we can note that dimensionless flux corresponding to pattern A and C is much larger than that corresponding to pattern B or D, while it is almost the same for pattern B and D, and it owns the maximum value in the pattern of A. In Fig.5(c), it can be found that the mixing parameter $\mathrm{Mix}_{\rm eff}$ corresponding to pattern A or C is higher than that corresponding to pattern B or D, and it has the maximum value in the pattern of A.

Combining Fig.5(b) with 5(c), among the four patterns shown in Fig.2, we can see that pattern A has the highest capability of sample transport but the lowest capability of sample mixing, pattern C has moderate capability of sample transport and mixing, pattern B and D have very high capability of sample mixing, but their capability of sample transport is very low. In addition, it has been found that $(Q(D) - Q(B))/Q(B) = -0.00171$ and

$$\mathrm{Mix}_{\rm eff}(D) - \mathrm{Mix}_{\rm eff}(B))/\mathrm{Mix}_{\rm eff}(B) = 0.039475412\,,$$

where, $Q(D)$ represents the dimensionless flux corresponding to the pattern of D, and other parameters are defined in the same way. The above numerical simulation shows that the capability of sample transport and mixing corresponding to pattern B is much higher than that corresponding to pattern D at a percent of 0.17 and 3.94 respectively. In general, the capability of sample transport and mixing corresponding to pat-

tern B is the highest, which means that the curved microchannel has an optimized capability of sample mixing and transport when the heterogeneous surface is located at the left conjunction between the curved and straight part.

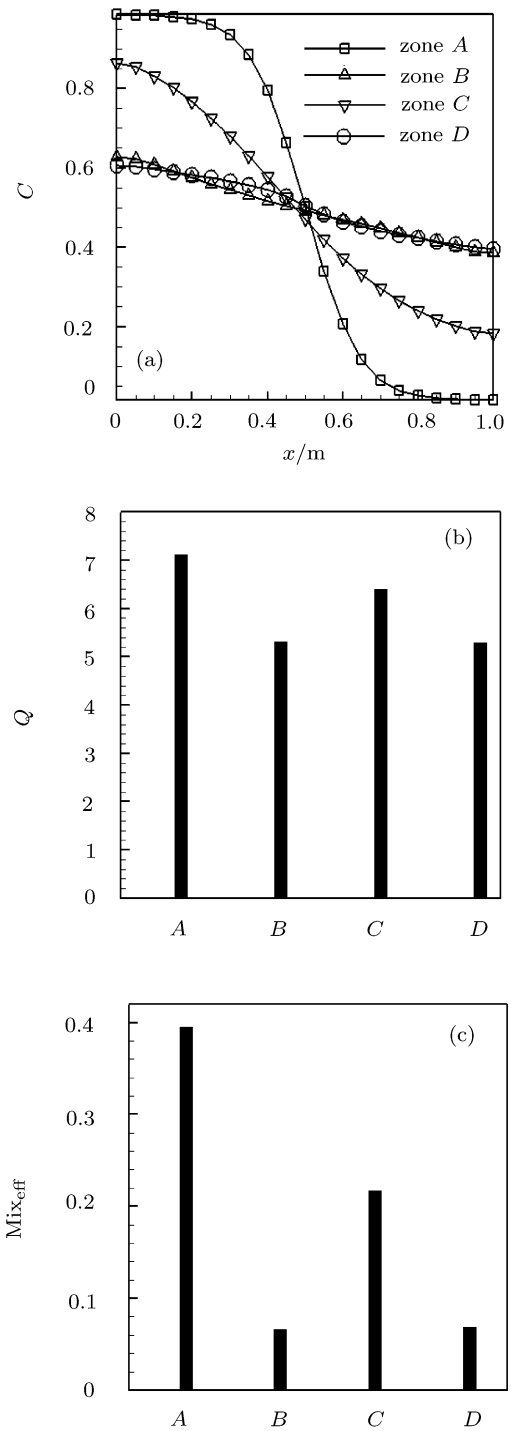


Fig.5. When r:W = 5 : 1 and $\psi_{\rm n}$ = −0.25 V, the relation between the pattern of heterogeneous surface and (a) the distribution of sample concentration at the outlet, (b) the dimensionless flux and (c) the dimensionless mixing parameter are given out respectively.

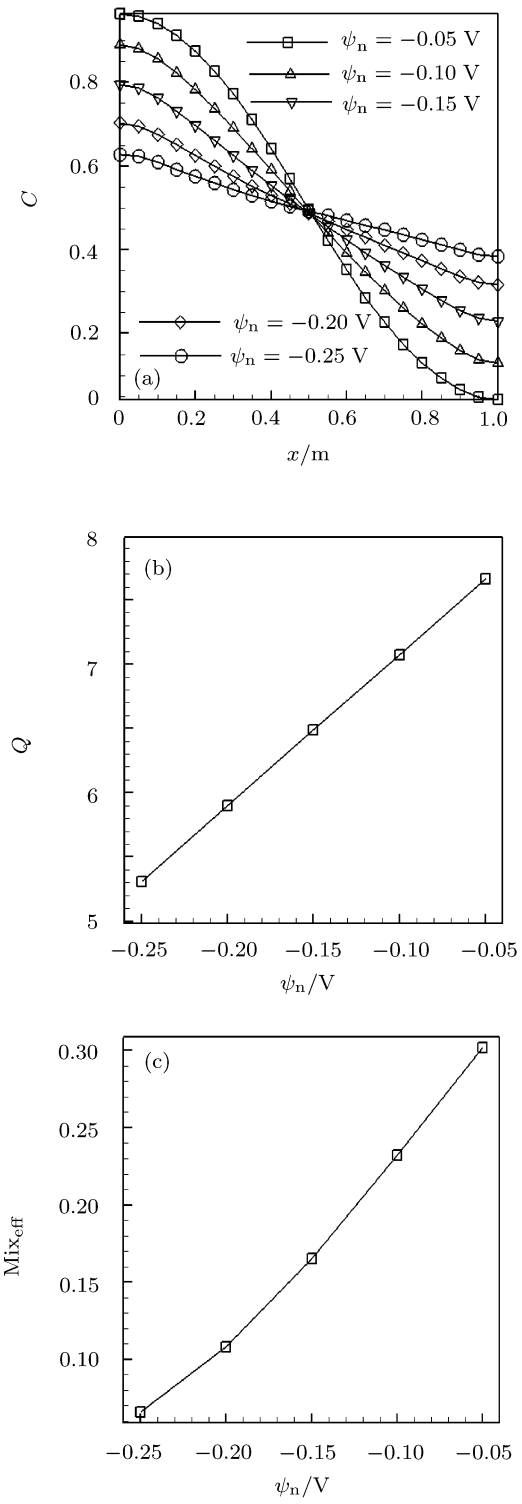


Fig.6. When r:W = 5 : 1 and the heterogeneous surface has the pattern of B, the relation between ψ_n and (a) the distribution of sample concentration at the outlet, (b) the dimensionless flux and (c) the dimensionless mixing parameter are given out respectively.

Referring to Fig.6(a), we can note that the con-

centration of sample at the outlet becomes more uniform with the decreasing of ψ_n, and it is uniform enough for a sufficient sample mixing when ψ_n is less than -0.2 V. As shown in Fig.6(b), it can be seen that the dimensionless flux decreases linearly with the decreasing of ψ_n, that is because of the reduction of the net charge for electroosmosis in this condition. In Fig.6(c), it can be noticed that the mixing parameter $\mathrm{Mix_{eff}}$ decreases moderately with the decreasing of ψ_n, which means a higher capability of sample mixing, while the capability of sample transport decreases linearly at the same time as shown in Fig.6(b).

In addition, when ψ_n changes from -0.25 V to -0.05 V, it has been known through numerical computation that the capability of sample transport has an enhancement at a percent of 44.3, while its capability of sample mixing decreases at a percent of 358. As a result, it can be concluded that the variation of heterogeneous surface potential ψ_n has more effect on the capability of sample mixing than on that of sample transport. That is why the relation between ψ_n and dimensionless flux should be considered first for the optimization of the curved microchannel for higher efficiency of sample mixing.

As shown in Fig.7(a), it can be noted that the concentration of sample at the outlet becomes very uniform when r:W is larger enough. Referring to Fig.7(b), we can see that the dimensionless flux decreases with the increasing of r:W and this trend becomes mild so that there is a reversely proportional relation between the intensity of electric field and r:W. At the same time, the intensity of circular region is proportional to the intensity of electric field. Thus, in the view of the intensity of circular region, the capability of sample mixing will decrease with the increasing of r:W, but it is opposite for that of sample transport. On the other hand, according to the definition of pattern D, it can be found that the size of the circulation region is proportional to r:W. As a result, the capability of sample mixing increases with the increasing of r:W because of larger intensity of the circulation region.

From the aforementioned analysis, it can be seen that r:W has positive and negative influence on the capability of sample mixing, and the integrative influence can be noticed from Fig.7(c), the mixing parameter $\mathrm{Mix_{eff}}$ increases first and then decreases moderately with the increasing of r:W, and the dividing point is r:$W = 3:1$. In addition, it can also be noted that the sample have achieved a sufficient mixing when r:W is larger than 5.

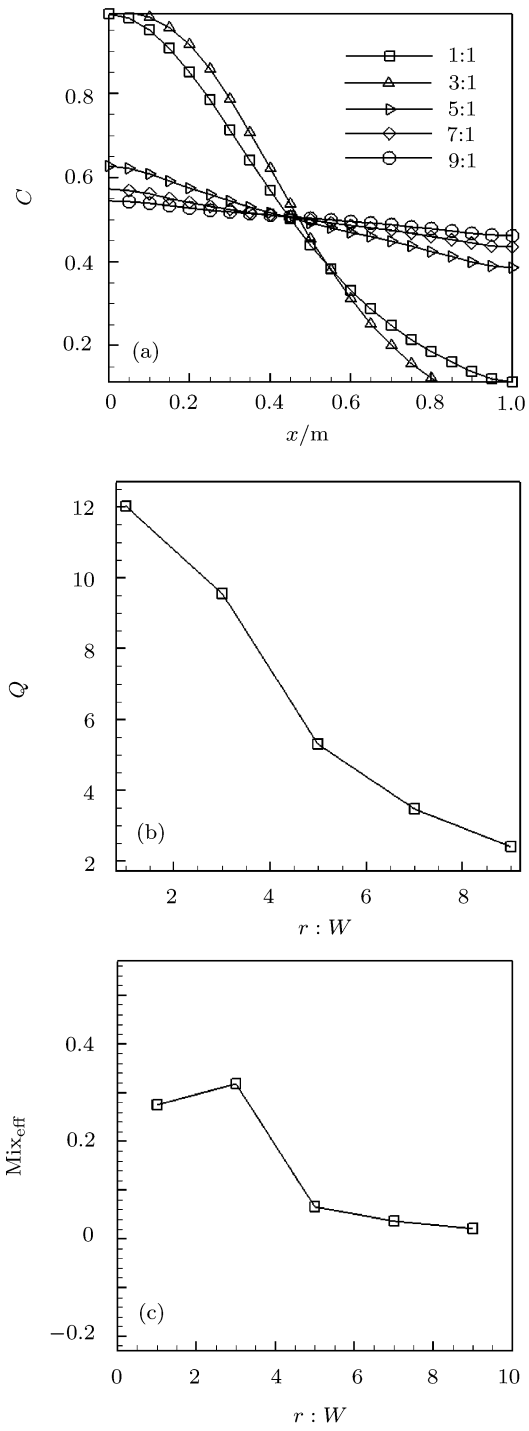


Fig.7. When $\psi_n = -0.25$ V and the heterogeneous surface has the pattern of B, the relation between r:W and (a) the distribution of sample concentration at the outlet, (b) the dimensionless flux and (c) the dimensionless mixing parameter are given out respectively.

Combining Fig.7(b) with Fig.7(c), when r:W changes from 1 to 9, we can know through numerical computation that the capability of sample transport

has a reduction at a percent of 80, while its capability of sample mixing has an enhancement at a percent of 92, which means that the ratio of the curved microchannel's radius to width has a comparable effect on the capability of sample mixing and transport. As a result, it can be said that the variation of r:W is not very important for the optimization of sample mixing in the microchannel.

4. Conclusions

Sample mixing and transport in 2D curved microchannels with heterogeneous surface potentials was analysed numerically by using the control-volume-based finite difference method. The results show that the curved microchannel has an optimized capability of sample mixing and transport when the heterogeneous surface is located at the left conjunction between the curved part and straight part. The variation of heterogeneous surface potential $\psi_{\rm n}$ has more effect on the capability of sample mixing than on that of sample transport. The ratio of the curved microchannel's radius to width has a comparable effect on the capability of sample mixing and transport. The conclusions above can be utilized in the optimization of the design of microfluidic devices for improving of the efficiency of sample mixing.

References

[1] Chang C C and Yang R J 2004 *J. Micromech. Microeng.* **14** 550

[2] Liu Y Z, Byoung J K and Hyung J S 2004 *Inter. J. Heat and Fluid Flow* **25** 986

[3] Joshua I M, Amy E H, Bruce P M, Juan G S and Thomas W K 2001 *Anal. Chem.* **73** 1350

[4] Liu R H and Mark A S 2000 *J. Microelectromechanical Systems* **9** 190

[5] Gao X Y, Zhao X P and Zheng C Q 2000 *Acta Phys. Sin.* **49** 272 (in Chinese)

[6] Zhao X P and Gao D J 2001 *Acta Phys. Sin.* **50** 1115 (in Chinese)

[7] Ajdari A 1995 *Phys. Rev. Lett.* **75** 755

[8] Ajdari A 1995 *Phys. Rev.* E **53** 4996

[9] Fu L M, Lin J Y and Yang J R 2003 *J. Colloid Interface Sci.* **258** 266

[10] Stroock A D, Weck M, Chiu D T, Huck W T S, Kenis P J A, Ismagilov R F and Whitesides G M 2000 *Phys. Rev. Lett.* **84** 3314

[11] Erickson D and Li D 2002 *Langmuir* **18** 1883

[12] Oddy M H, Santiago J G and Mikkelsen J C 2001 *Anal. Chem.* **73** 5822

[13] Hao L, Brian D S and Michael H O 2004. *Phys. Fluids* **16** 1922

[14] Tian F Z, Li B M and Daniel Y K 2005 *Langmuir* **21** 1126

[15] Li Z H, Lin J Z and Nie D M 2005 *Appl. Math. Mech.* **26** 685

[16] Zhang K, Lin J Z and Li Z H 2006 *Appl. Math. Mech.* **5 27** 575